An experimental and modeling study of ammonia with enriched oxygen content and ammonia/hydrogen laminar flame speed at elevated pressure and temperature

Krishna Prasad Shrestha[1*], Charles Lhuillier[2,3], Amanda Alves Barbosa[2], Pierre Brequigny[2], Francesco Contino[3], Christine Mounaïm-Rousselle[2], Lars Seidel[4*], Fabian Mauss[1]

1. Thermodynamics and Thermal Process Engineering, Brandenburg University of Technology, Siemens-Halske-Ring 8, 03046 Cottbus, Germany
2. Univ. Orléans, INSA-CVL, PRISME, EA 4229, F45072, Orléans, France
3. Thermo and Fluid Dynamics (FLOW), Vrije Universiteit Brussel, Belgium
4. LOGE Deutschland GmbH, Burger Chaussee 25, 03044 Cottbus, Germany

Proc. Combust. Inst. 38, 2020

https://doi.org/10.1016/j.proci.2020.06.197

Corresponding author: Lars Seidel, e-mail: lars.seidel@logesoft.com

Krishna Prasad Shrestha, e-mail: shrestha@b-tu.de, ORCID: 0000-0001-5672-7354

Supporting Information

1. NH_3 and NH_3/H_2 laminar flame speed

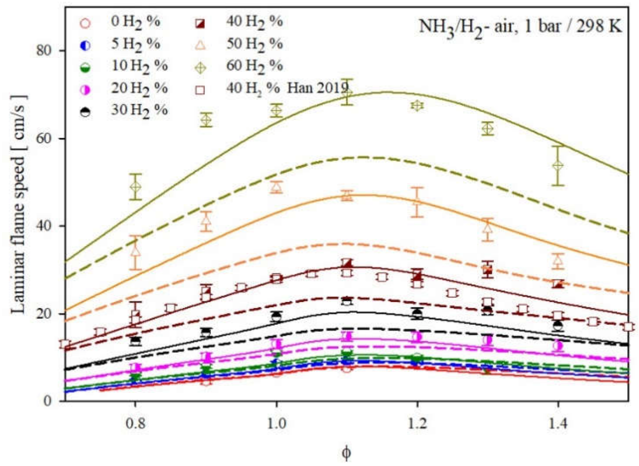

Figure S1: Laminar flame speed of NH_3/H_2/air at different NH_3/H_2 blending ratio (0-60 %) at 1 bar and 298 K. Symbols experiments from [1], Solid lines: this work, Dashed lines: previous model [2].

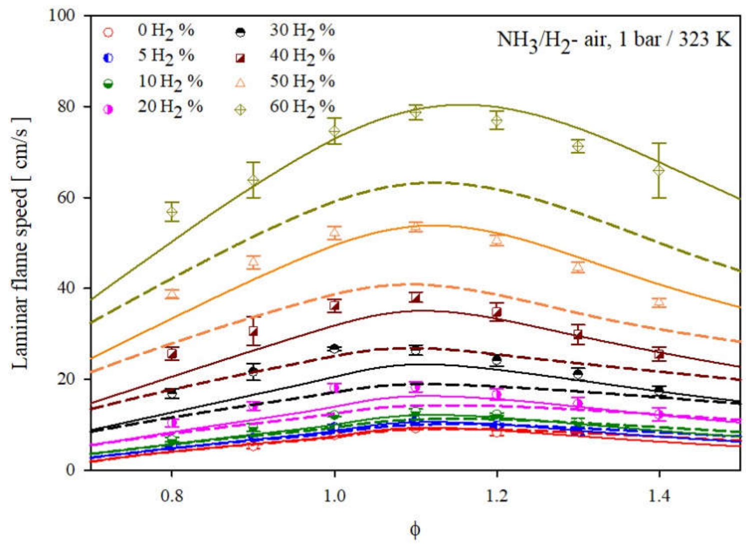

Figure S2: Laminar flame speed of NH_3/H_2/air at different NH_3/H_2 blending ratio (0-60 %) at 1 bar and 323 K. Symbols experiments from [1], Solid lines: this work, Dashed lines: previous model [2].

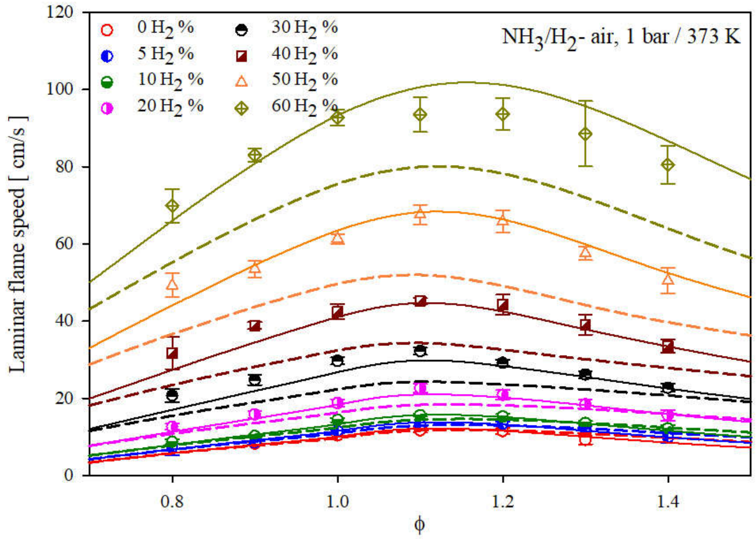

Figure S3: Laminar flame speed of NH_3/H_2/air at different NH_3/H_2 blending ratio (0-60 %) at 1 bar and 373 K. Symbols experiments from [1], Solid lines: this work, Dashed lines: previous model [2].

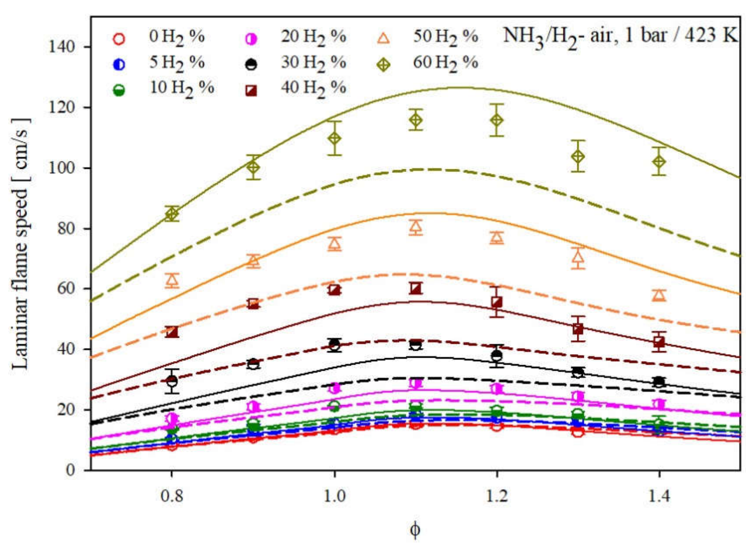

Figure S4: Laminar flame speed of NH_3/H_2/air at different NH_3/H_2 blending ratio (0-60 %) at 1 bar and 423 K. Symbols experiments from [1], Solid lines: this work, Dashed lines: previous model [2].

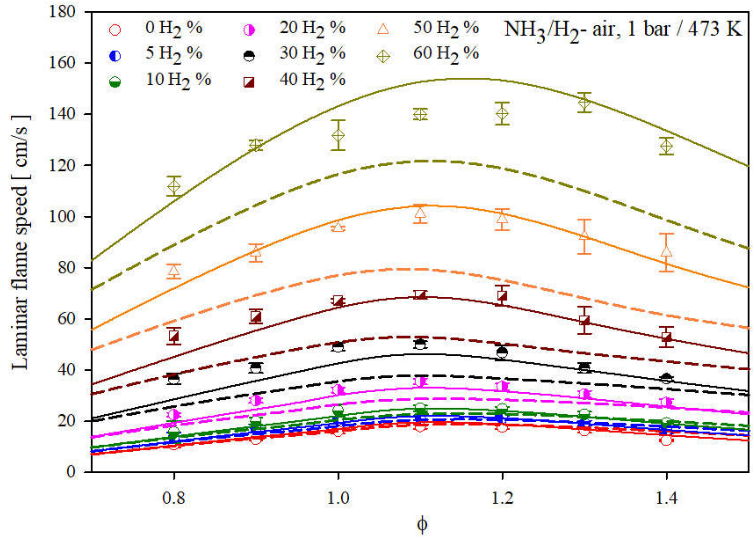

Figures S5: Laminar flame speed of NH_3/H_2/air at different NH_3/H_2 blending ratio (0-60 %) at 1 bar and 473 K. Symbols experiments from [1], Solid lines: this work, Dashed lines: previous model [2].

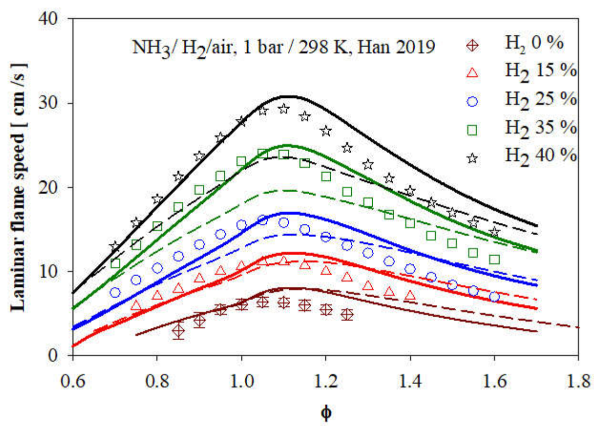

Figure S6: Laminar flame speed of NH_3/H_2/air at different NH_3/H_2 blending ratio (0-40 %) at 1 bar and 298 K. Symbols: experiments from [3], solid lines: present model, dashed lines: previous model [2].

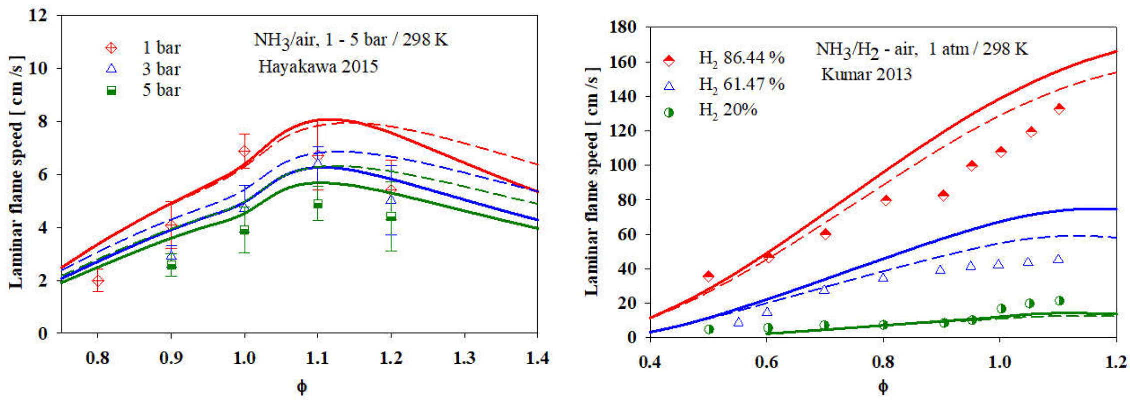

Figures S7: Laminar flame speed of NH_3/air (left) 1-5 bar, 298 K and NH_3/H_2/air (right) at 1 atm and 298 K. Symbols experiments from [4,5], solid lines: present model, dashed lines: previous model [2].

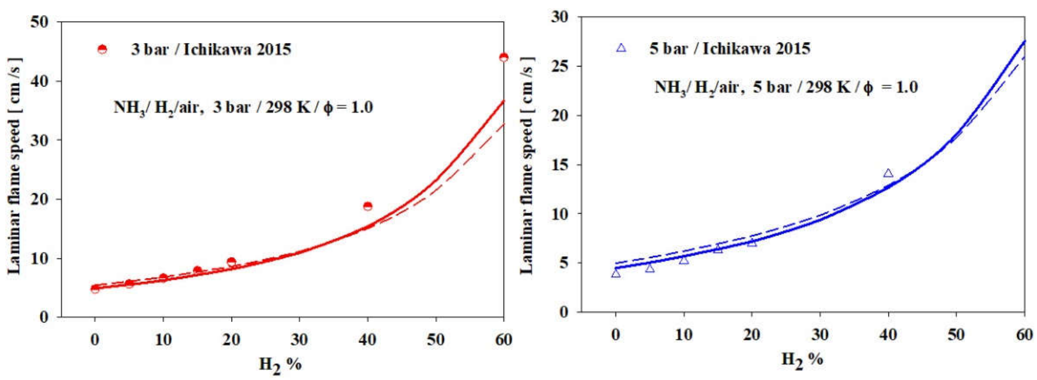

Figure S8**:** Laminar flame speed of NH_3/H_2/air at $\phi = 1.0$, 298 K, 3 bar(left) and 5 bar (right). Symbols experiments from [6], solid lines: present model, dashed lines: previous model [2].

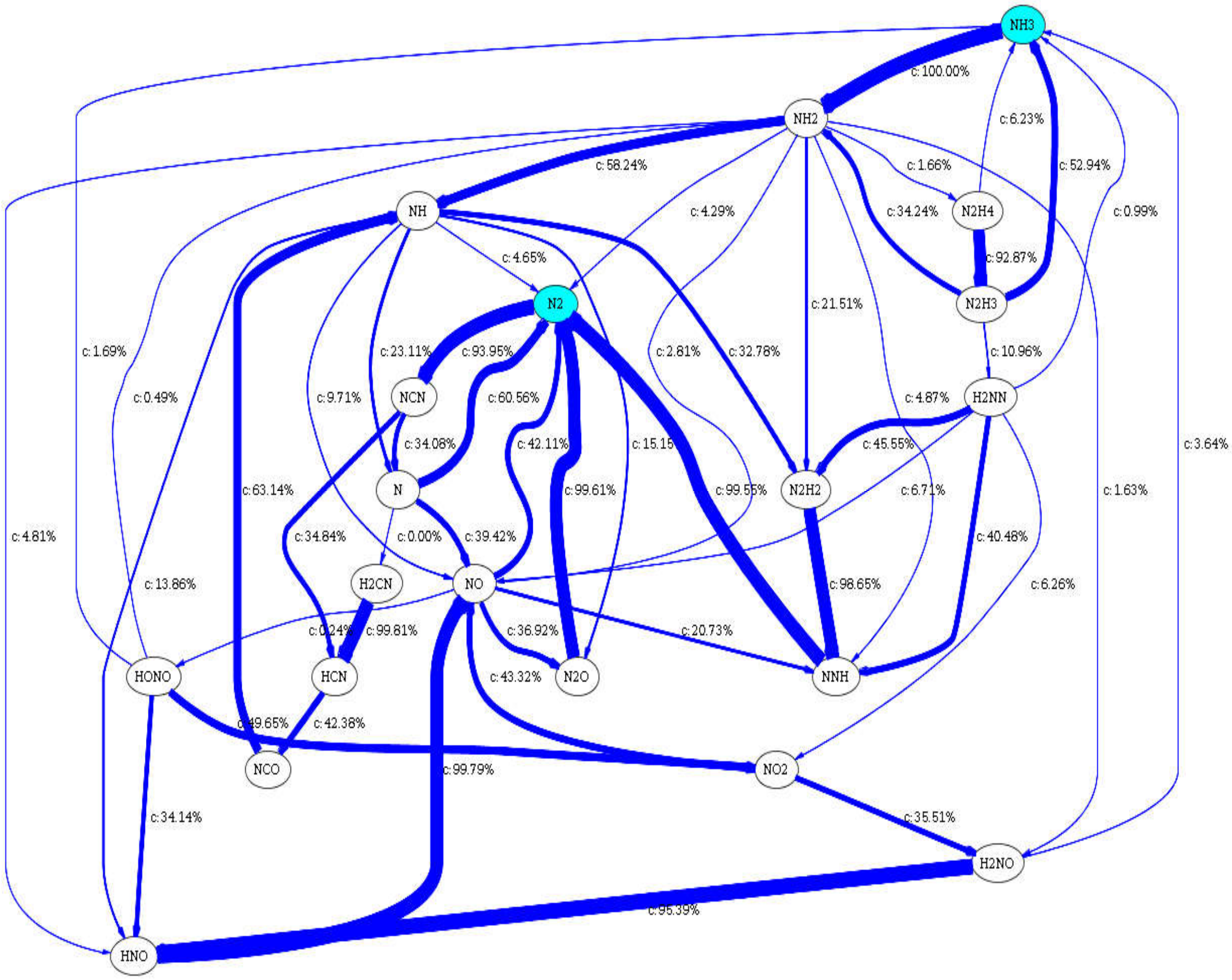

Figure S9: Reaction flow analysis based on N-atom for NH_3/H_2/air for 50 % H_2 in fuel blend at ϕ = 1.0, 1 bar and 298 K.

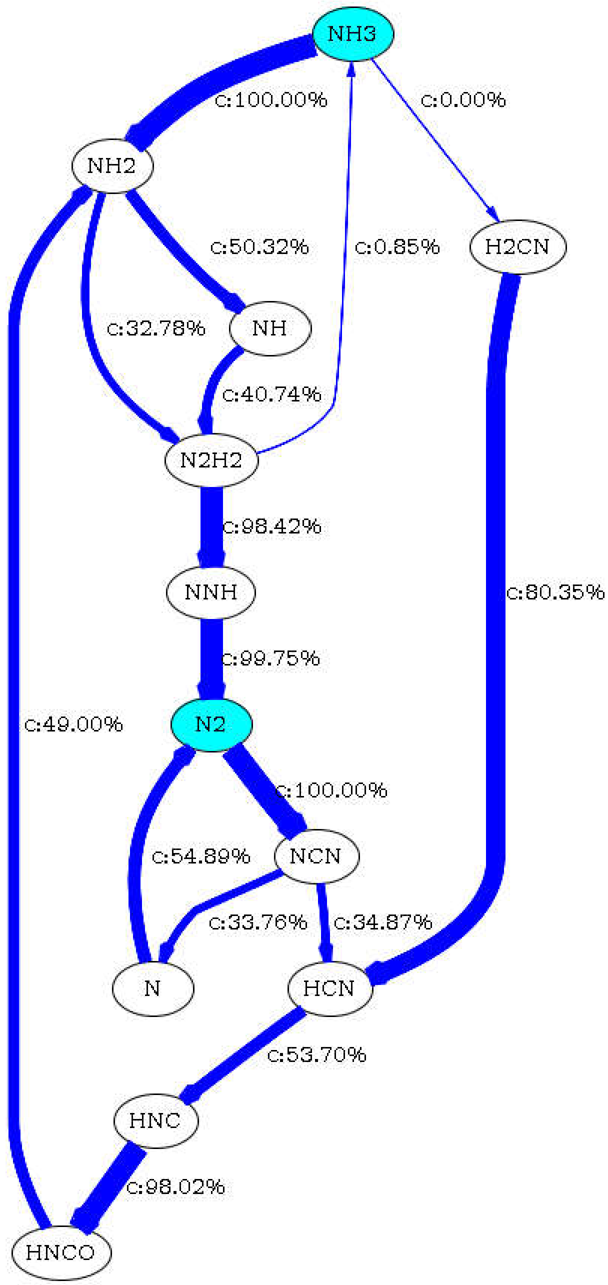

Figure S10: Reaction flow analysis based on N-atom for NH_3/air at ϕ = 1.0, 1 bar and 473 K.

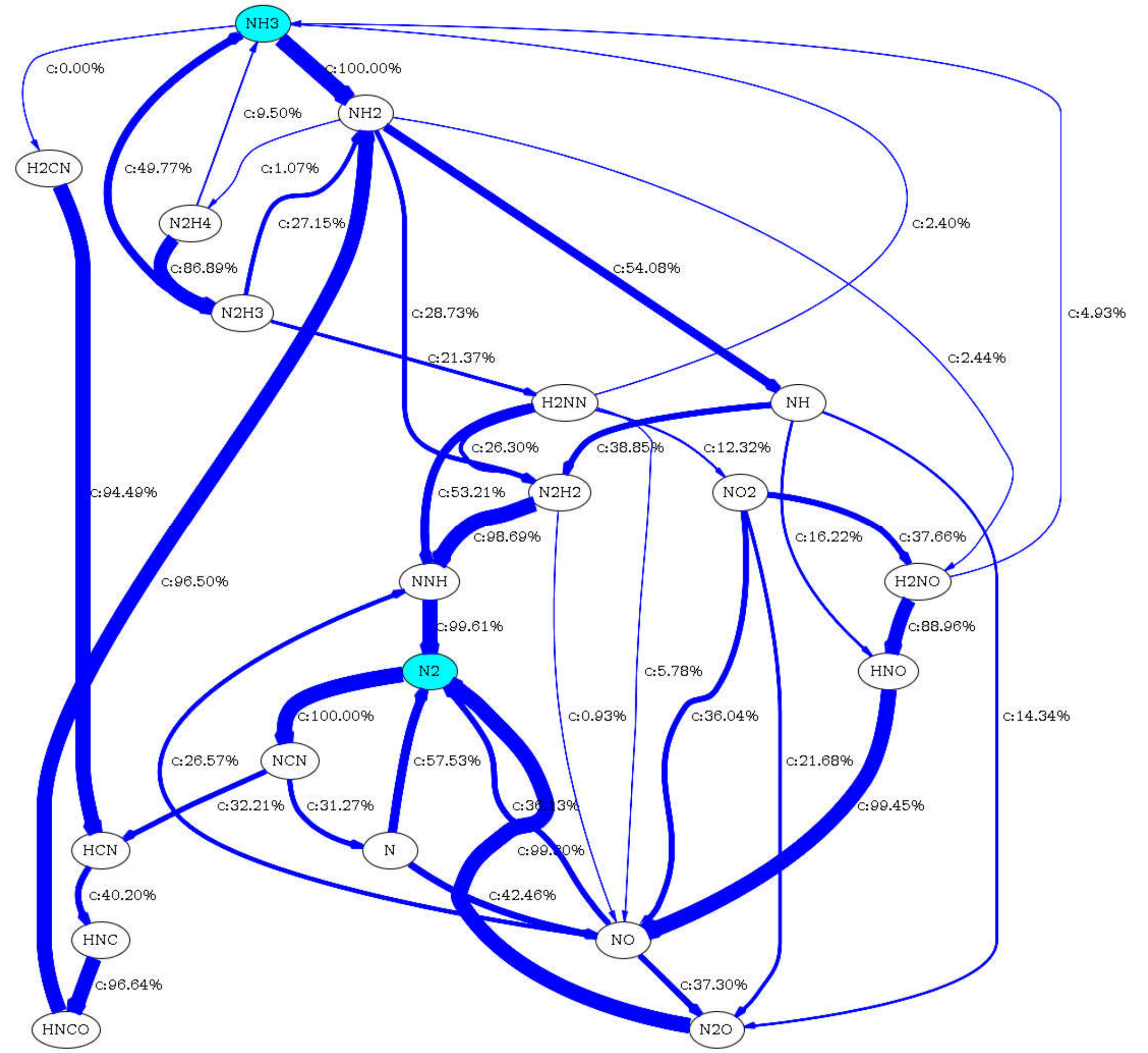

Figure S11: Reaction flow analysis based on N-atom for NH_3/H_2/air with 30 % H_2 at ϕ = 1.0, 1 bar and 473 K.

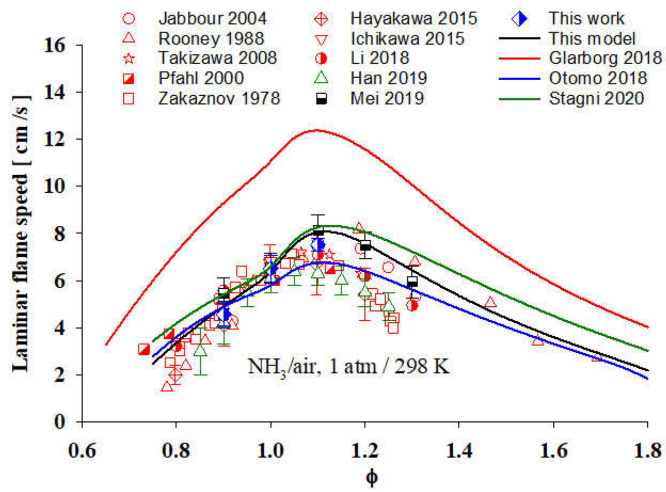

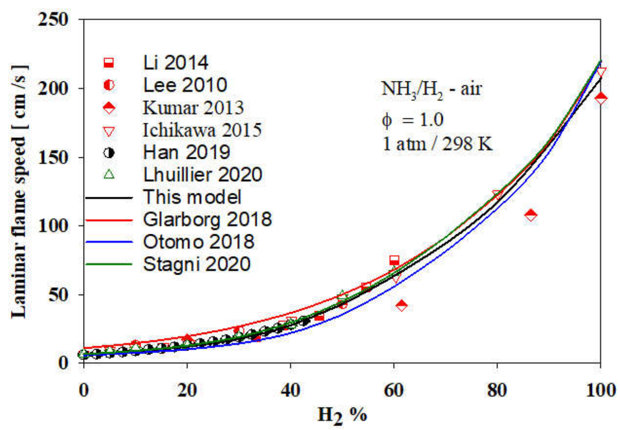

Figure S12: Laminar flame speed at 1 atm and 298 K for NH_3/air (a) and for stoichiometric conditions for NH_3/H_2/air (b). Symbols: measurements from this work and published literature [3,4,6–13]. Solid lines: model prediction; black (This model), Red (Glarborg et al. 2018 [14]), Blue (Otomo et al. 2018 [15]), Green (Stagni et al. 2020 [16]).

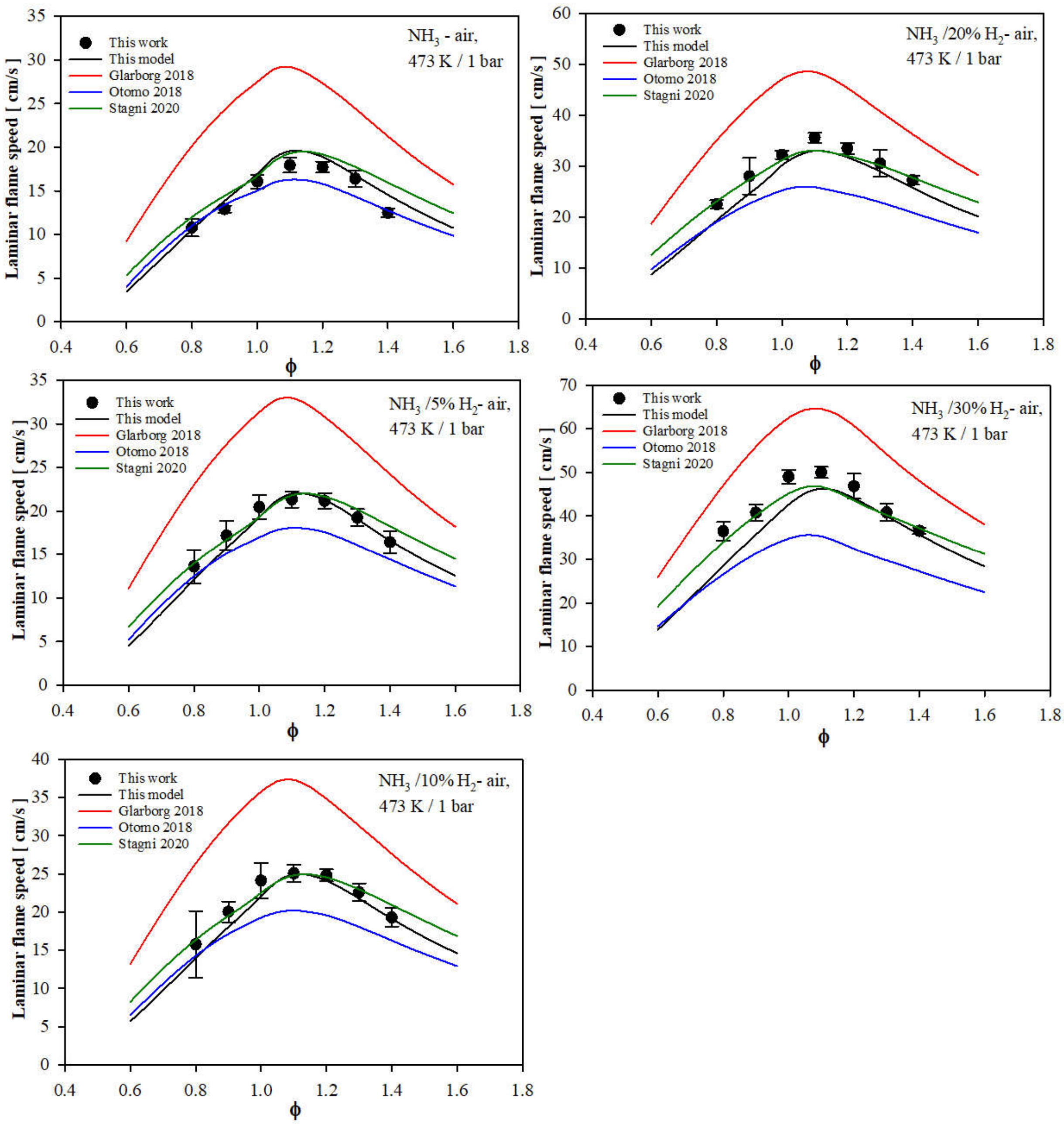

Figure S13: Laminar flame speeds of NH_3/H_2/air at 473 K and 1 bar at varying H_2 content. Symbols: measurements from this work. Solid lines: model prediction; black (This model), Red (Glarborg et al. 2018 [14]), Blue (Otomo et al. 2018 [15]), Green (Stagni et al. 2020 [16]).

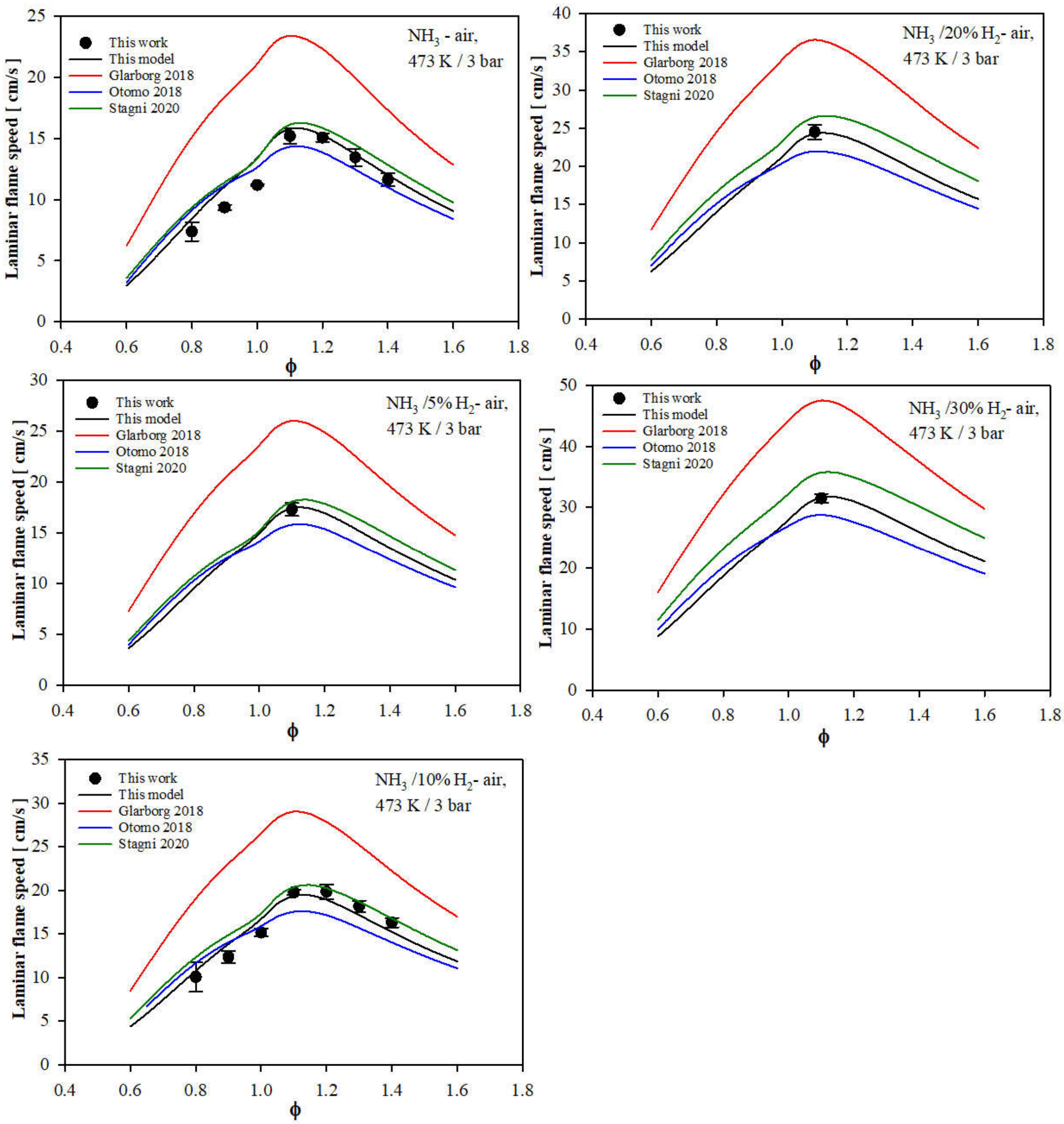

Figure S14: Laminar flame speeds of NH_3/H_2/air at 473 K and 3 bar at varying H_2 content. Symbols: measurements from this work. Solid lines: model prediction; black (This model), Red (Glarborg et al. 2018 [14]), Blue (Otomo et al. 2018 [15]), Green (Stagni et al. 2020 [16]).

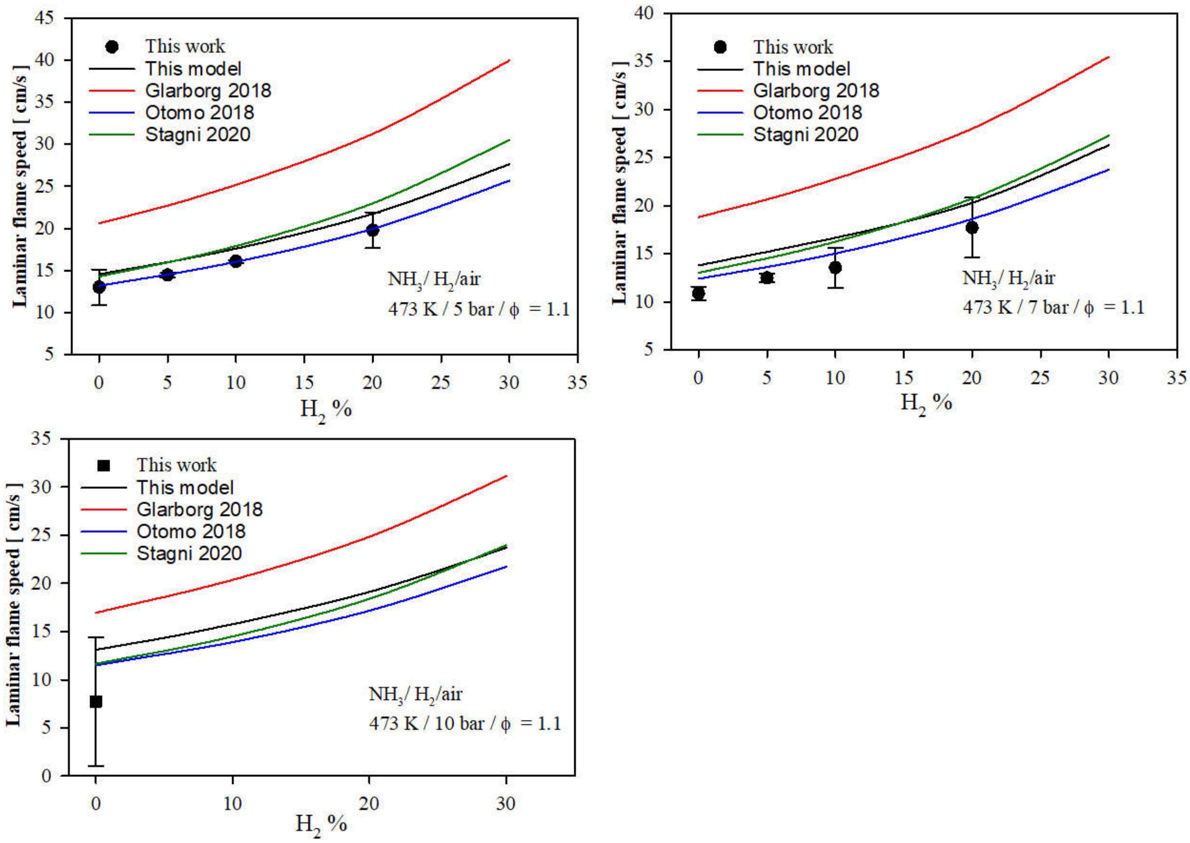

Figure S15: Laminar flame speed of NH_3/H_2/air at 473K and varying H_2 content at ϕ = 1.1 and 5, 7 and10 bar. Symbols: experiments this work. Solid lines: model prediction; black (present model), Red (Glarborg et al. 2018 [14]), Blue (Otomo et al. 2018 [15]), Green (Stagni et al. 2020 [16]).

2. NH_3 laminar flame speed with varying oxygen content

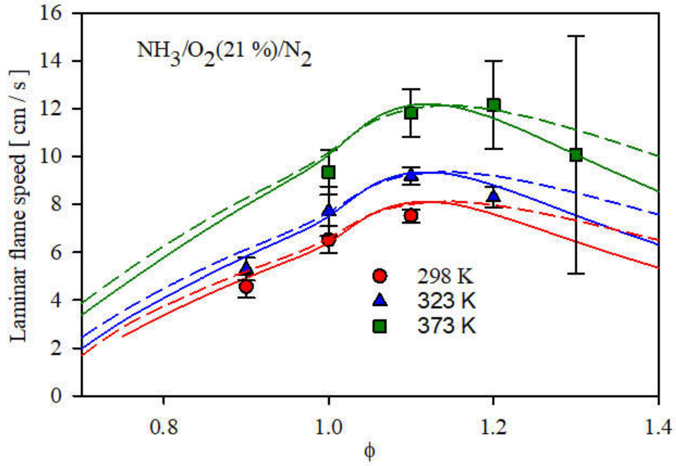

Figure S16: NH_3/air laminar flame speed at different temperature. Symbols: this work, solid lines: present model, dashed lines: previous model [2].

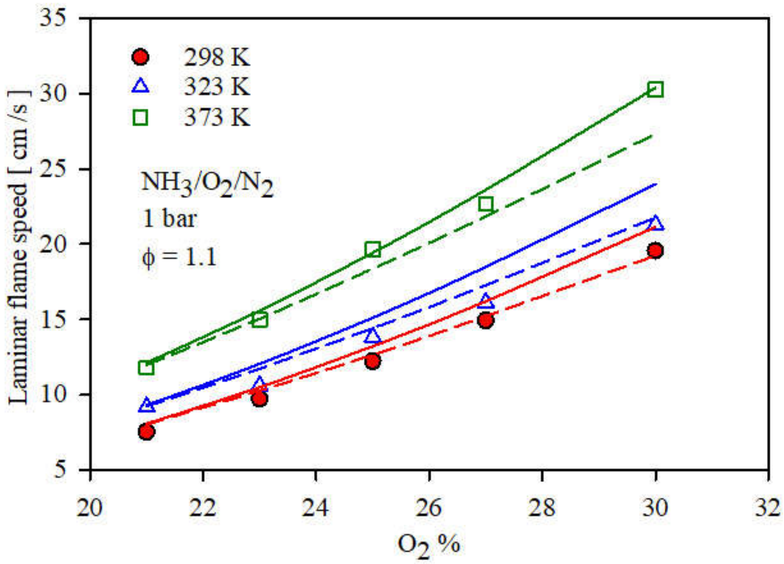

Figure S17: $NH_3/O_2/N_2$ laminar flame speed as function of O_2 variation at different temperature. Symbols: this work, solid lines: present model, dashed lines: previous model [2].

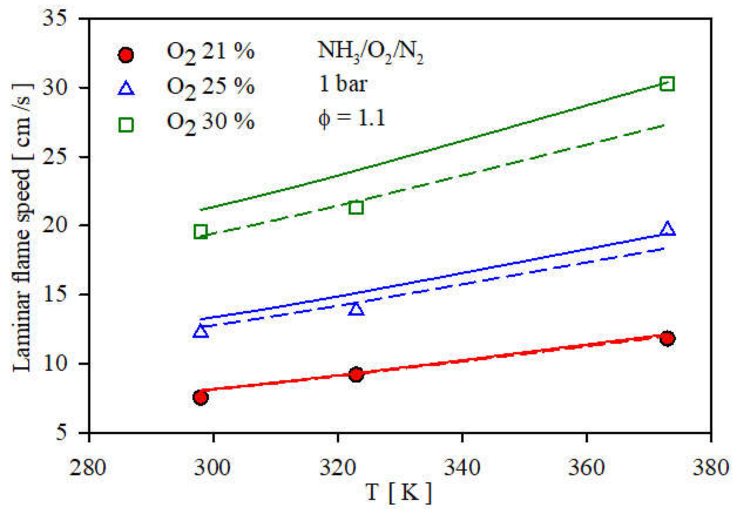

Figure S18: $NH_3/O_2/N_2$ laminar flame speed as function of temperature at different O_2 content. Symbols: this work, solid lines: present model, dashed lines: previous model [2].

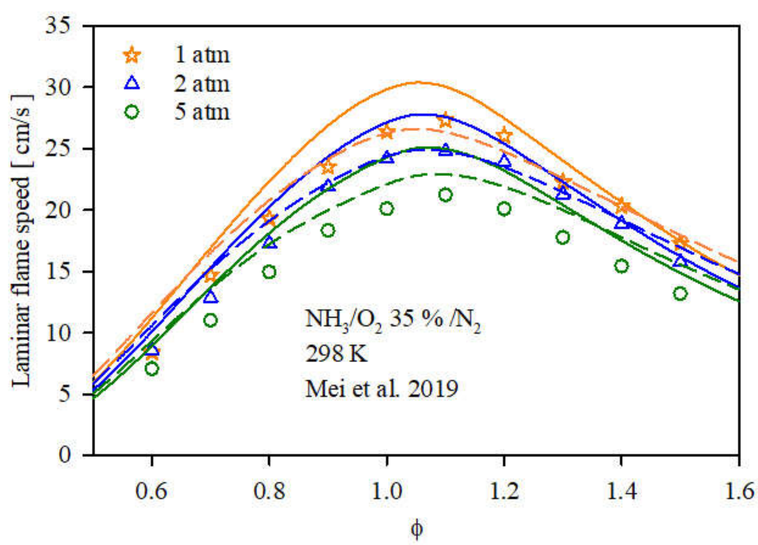

Figures S19: Laminar flame speed of NH_3/O_2(35 %)/N_2 at 1-5 atm, 298 K. Symbols experiments from [13], solid lines: present model, dashed lines: previous model [2].

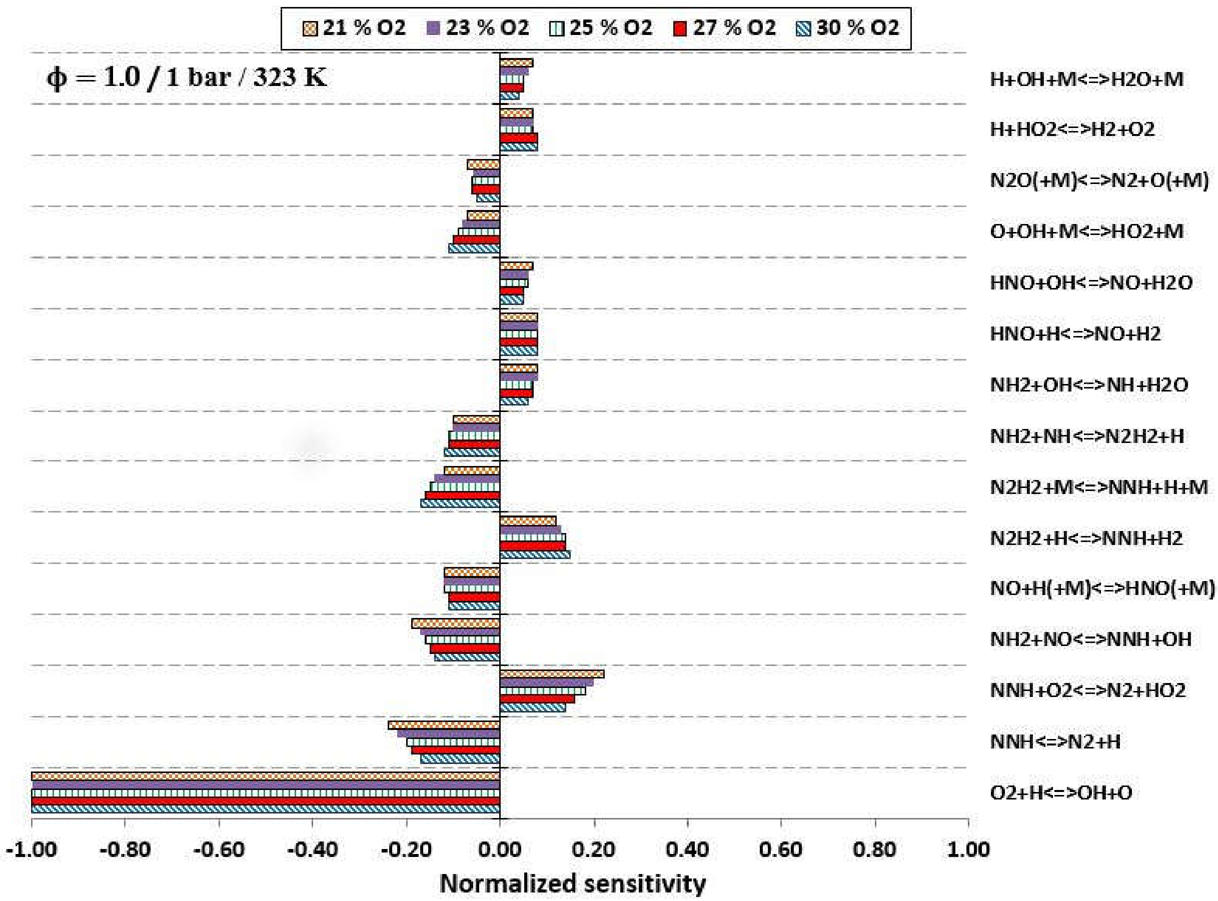

Figure S20: Normalized reaction sensitivity for laminar flame speed of $NH_3/O_2/N_2$ at ϕ = 1.0, 1 bar and 323 K with varying O_2 content.

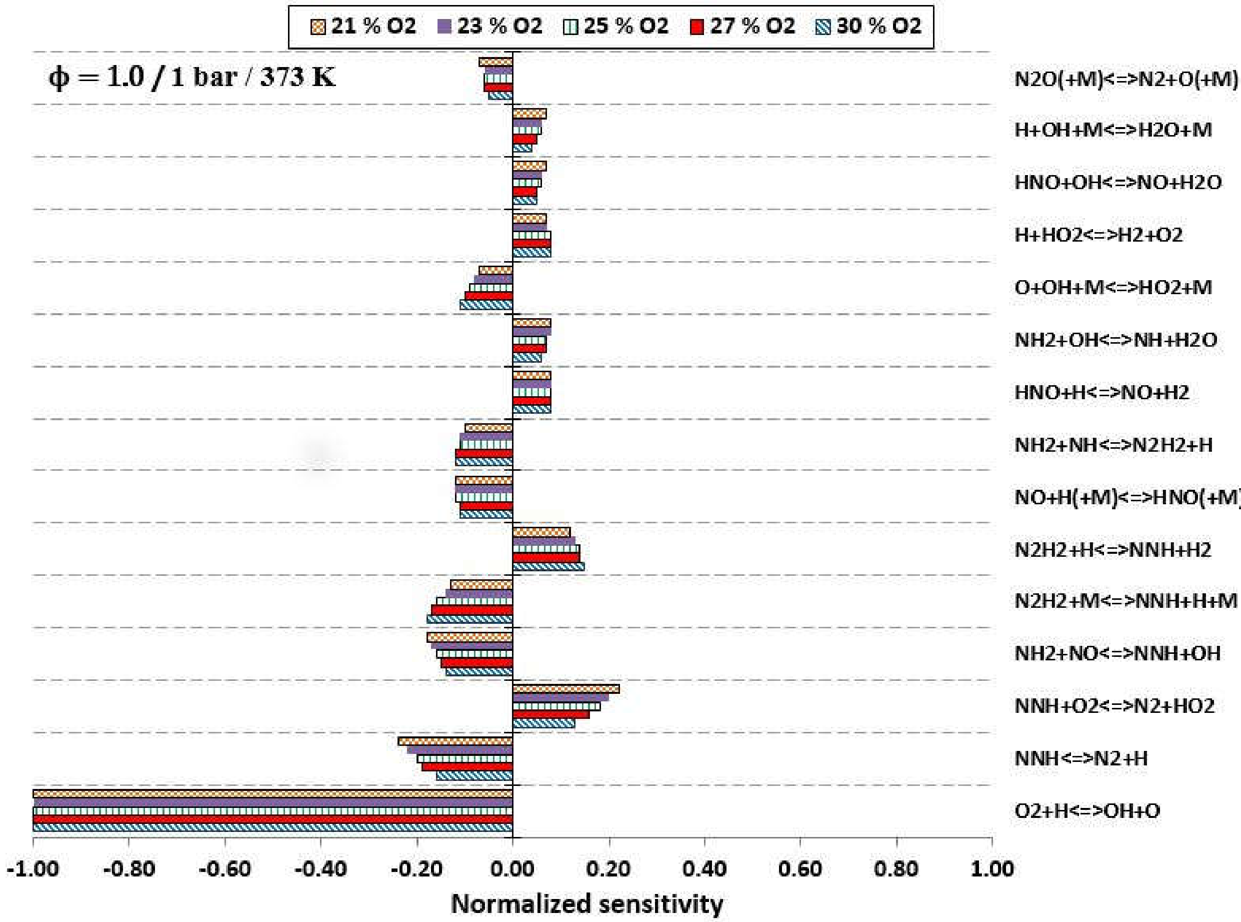

Figure S21: Normalized reaction sensitivity for laminar flame speed of $NH_3/O_2/N_2$ at ϕ = 1.0, 1 bar and 373 K with varying O_2 content.

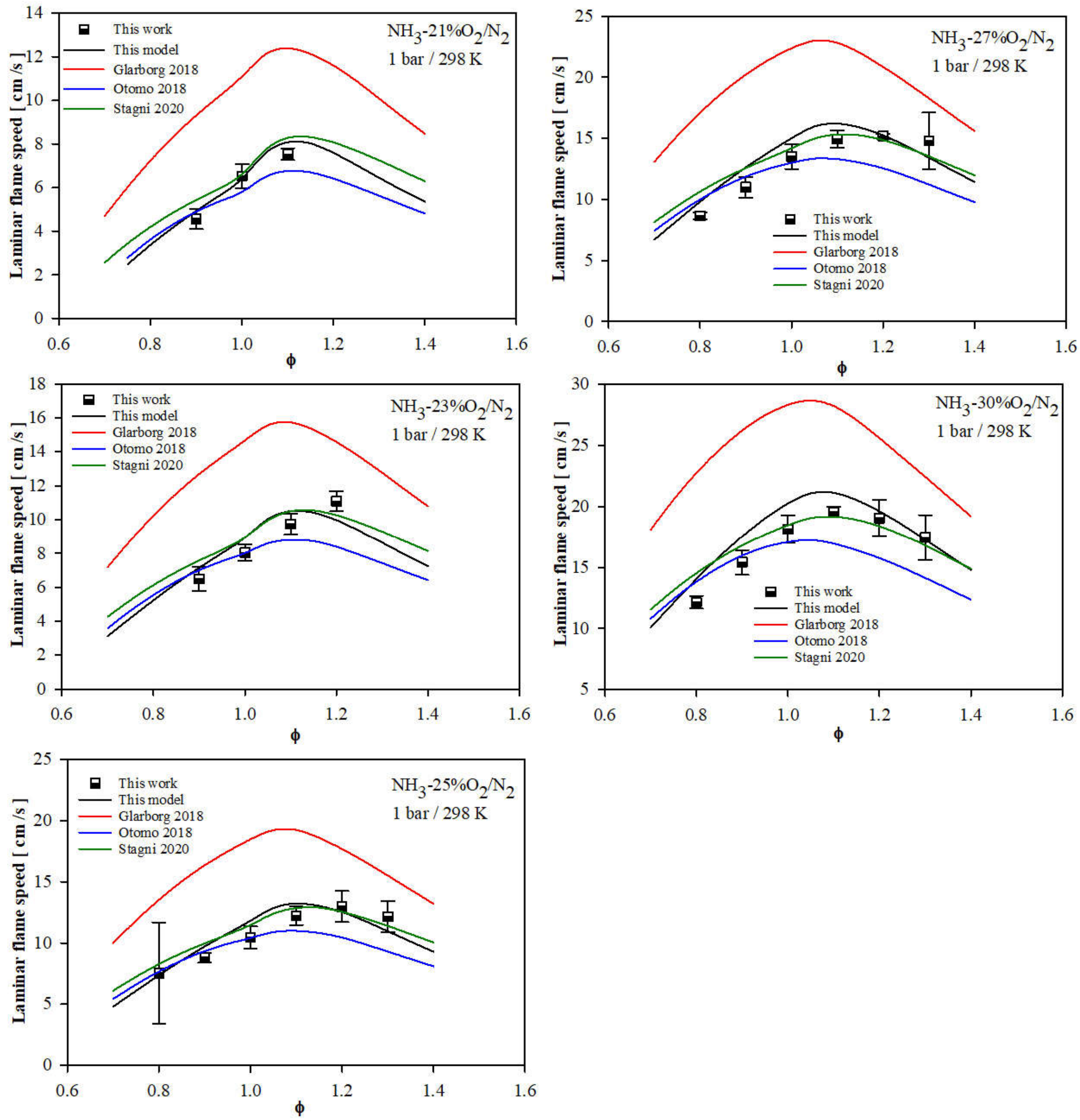

Figure S22: Laminar flame speed of $NH_3/O_2/N_2$ at 1 bar and 298 K with varying O_2 content (21 – 30%). Symbols: measurements from this work. Solid lines: model prediction; black (present model), Red (Glarborg et al. 2018 [14]), Blue (Otomo et al. 2018 [15]), Green (Stagni et al. 2020 [16]).

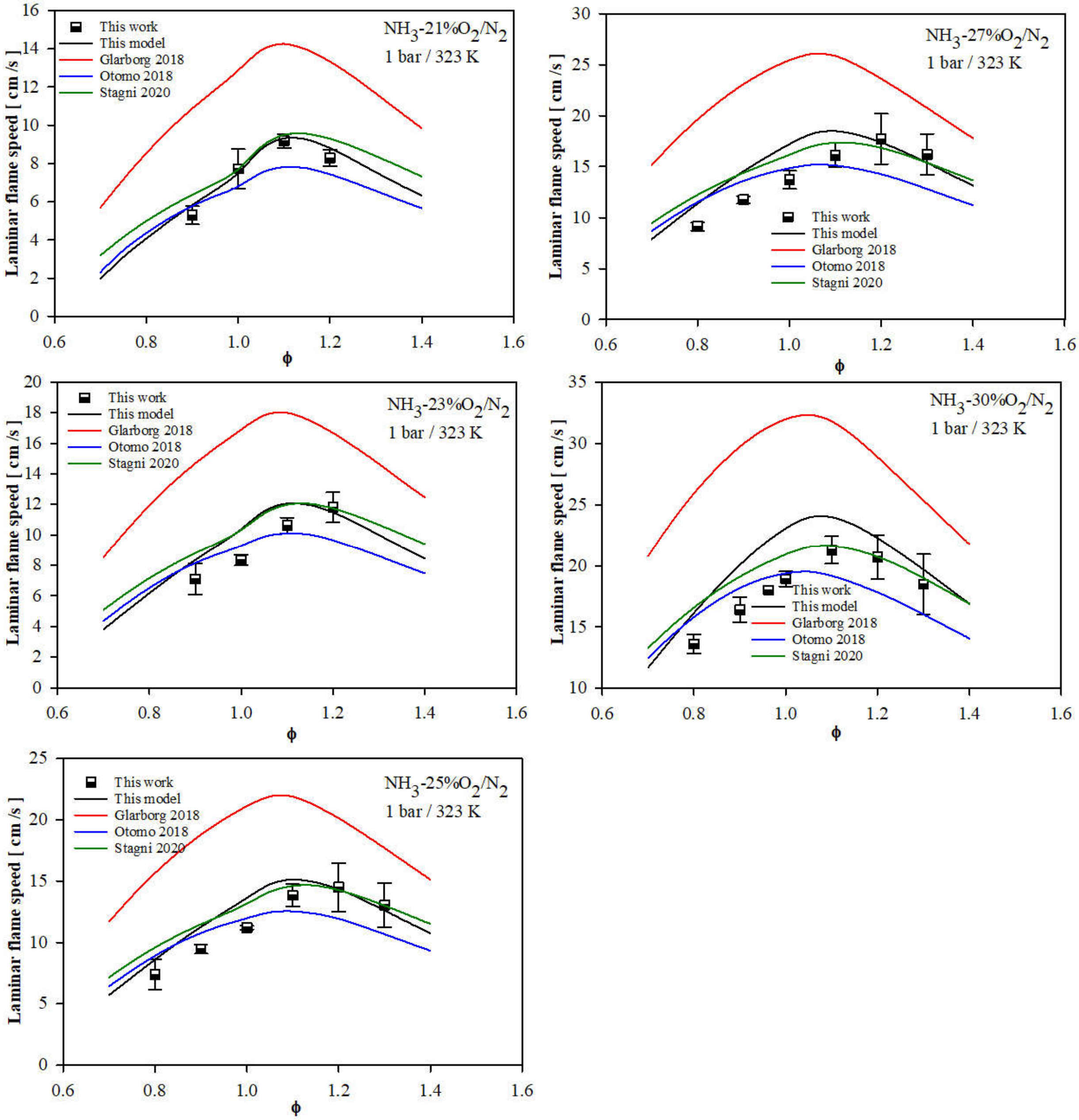

Figure S23: Laminar flame speed of $NH_3/O_2/N_2$ at 1 bar and 323 K with varying O_2 content (21 – 30%). Symbols: measurements from this work. Solid lines: model prediction; black (present model), Red (Glarborg et al. 2018 [14]), Blue (Otomo et al. 2018 [15]), Green (Stagni et al. 2020 [16]).

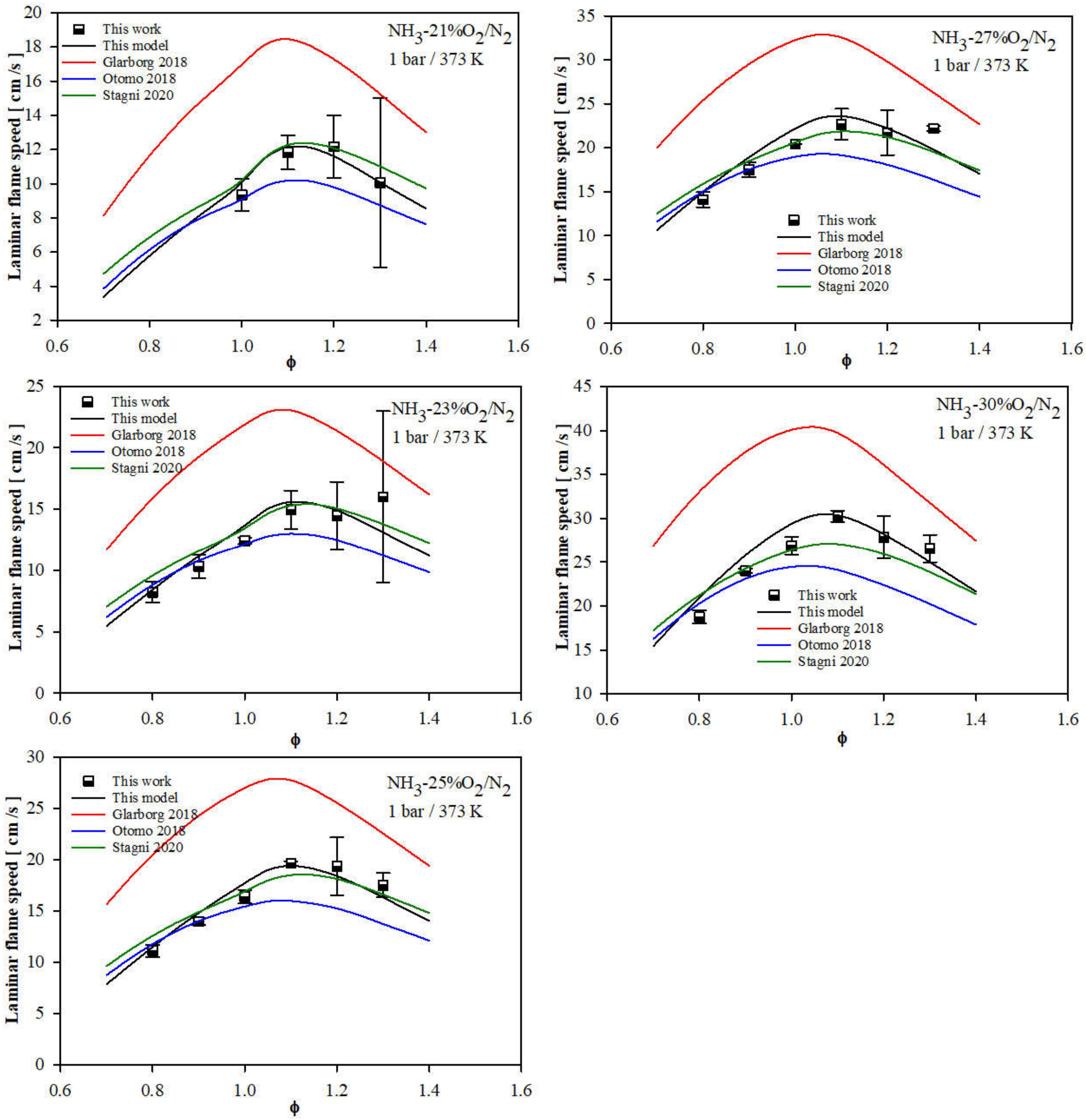

Figure S24: Laminar flame speed of $NH_3/O_2/N_2$ at 1 bar and 373 K with varying O_2 content (21 – 30%). Symbols: measurements from this work. Solid lines: model prediction; black (present model), Red (Glarborg et al. 2018 [14]), Blue (Otomo et al. 2018 [15]), Green (Stagni et al. 2020 [16]).

3. Ignition delay time

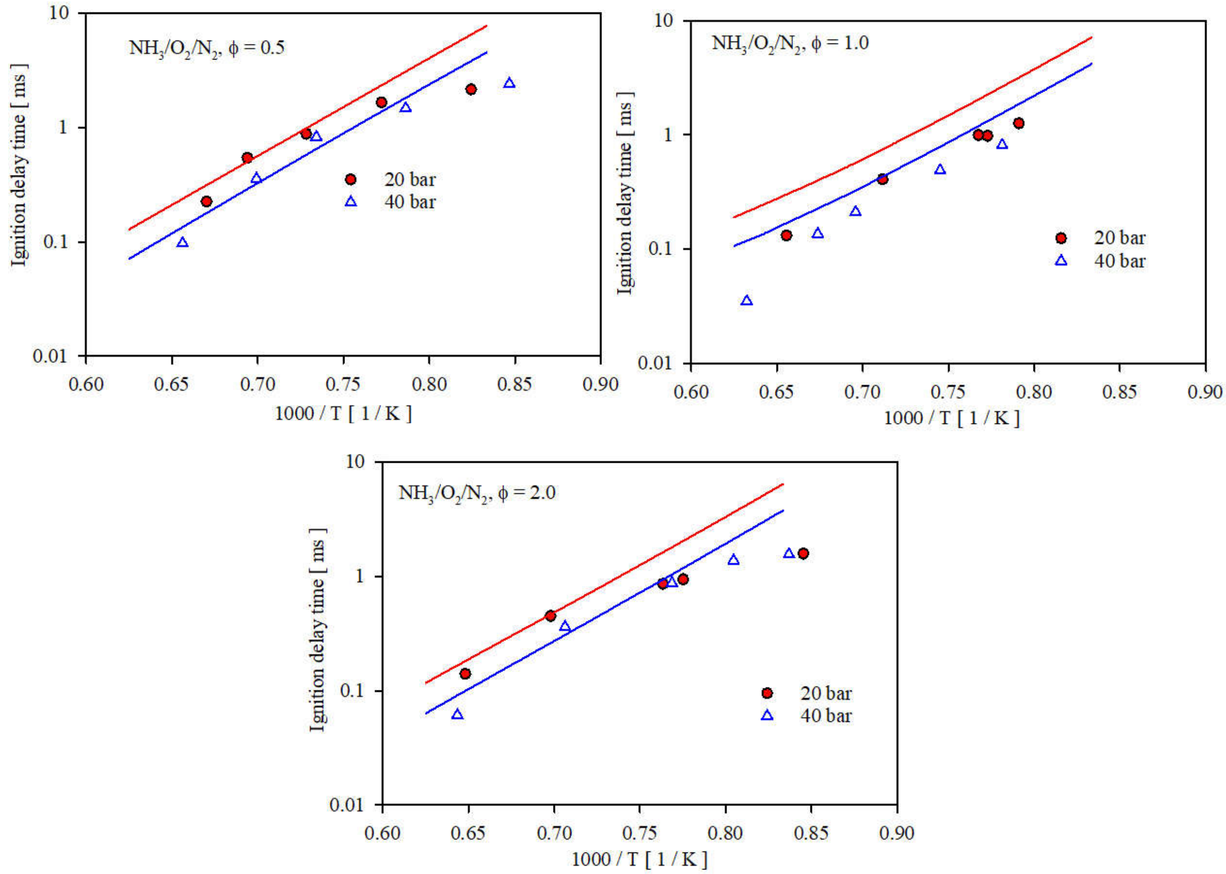

Figures S25: Ignition delay time of NH_3/air in shock tube at 20 and 40 bar for different ϕ. Symbols: experiments from [17], Lines: this work.

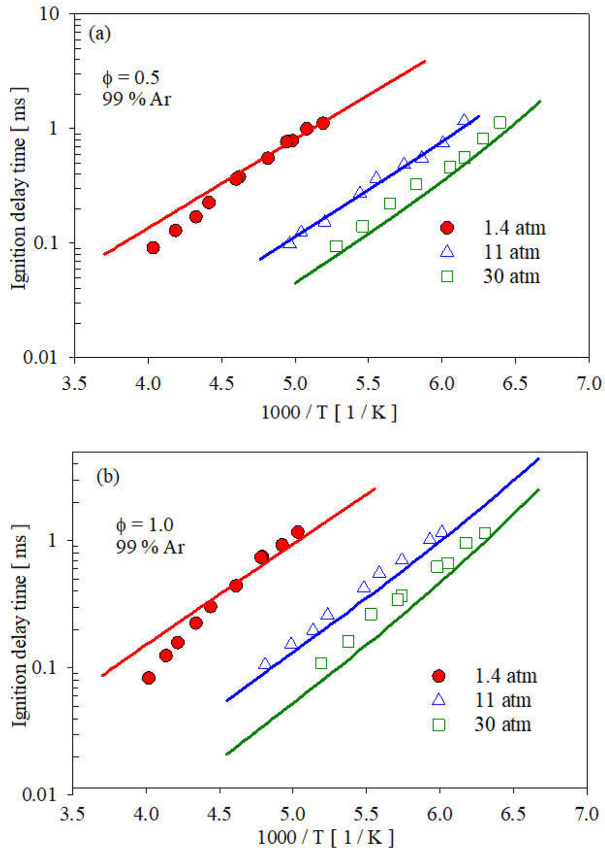

Figures S26: Ignition delay time of $NH_3/O_2/Ar$ in shock tube at 1.4-30 atm for different ϕ. Symbols: experiments from [18], Lines: this work.

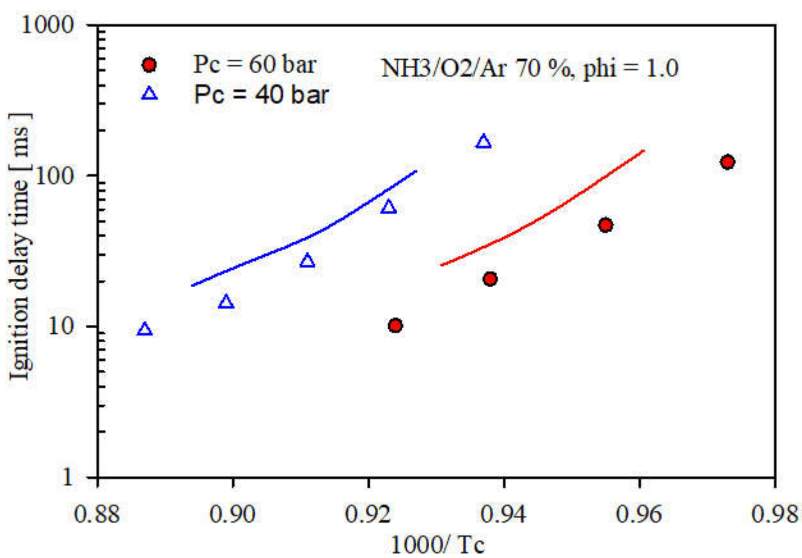

Figures S27: Ignition delay time of $NH_3/O_2/Ar$ in rapid compression machine at 60 and 40 bar for $\phi = 1.0$. Symbols: experiments from [19], Lines: this work.

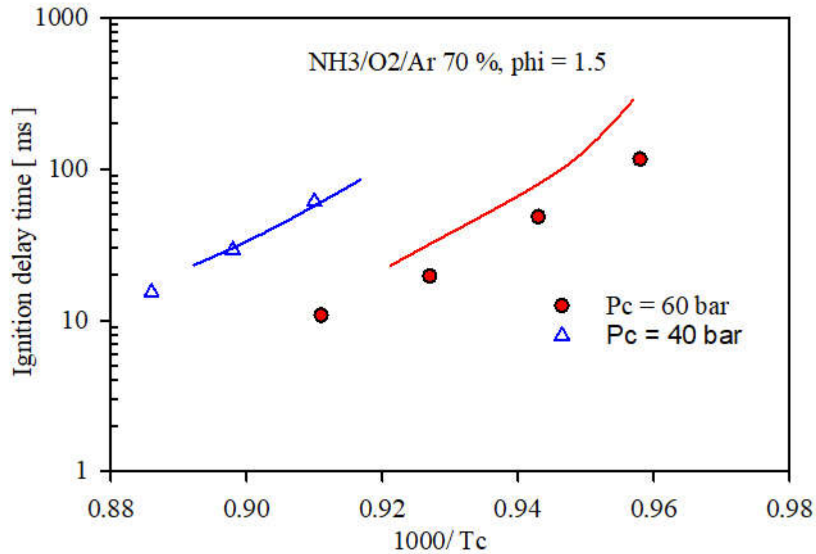

Figures S28: Ignition delay time of $NH_3/O_2/Ar$ in rapid compression machine at 60 and 40 bar for $\phi = 1.5$. Symbols: experiments from [19], Lines: this work.

4. Jet stirred reactor

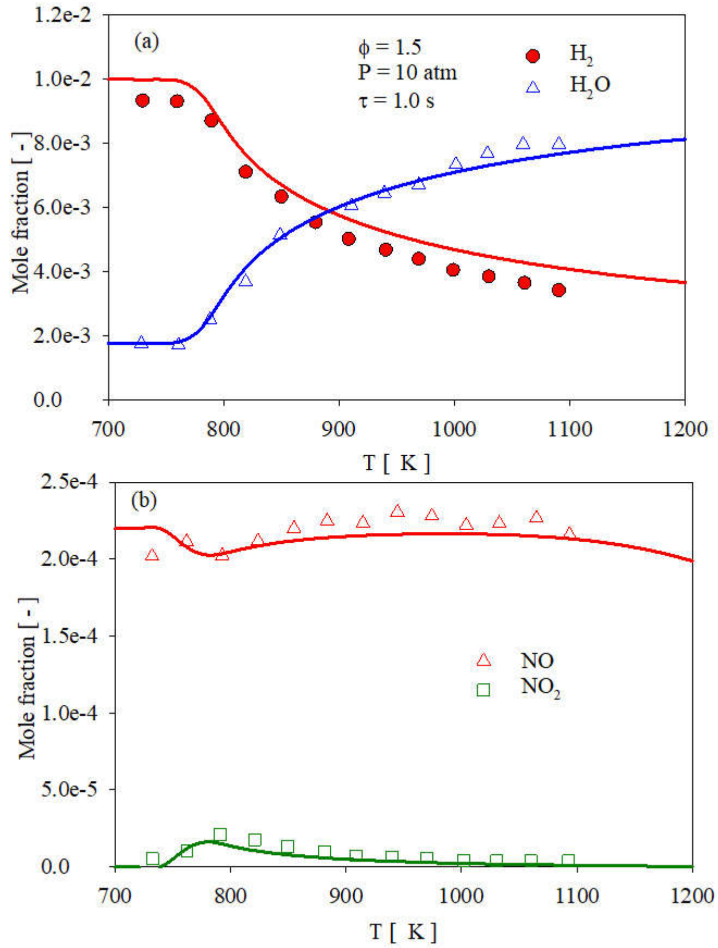

Figure S29**:** Speciation in during $H_2/O_2/N_2/NO$ oxidation in jet stirred reactor at ϕ = 1.5, 10 atm and τ = 1.0 s. Symbols: experiments from [20], Lines: this work

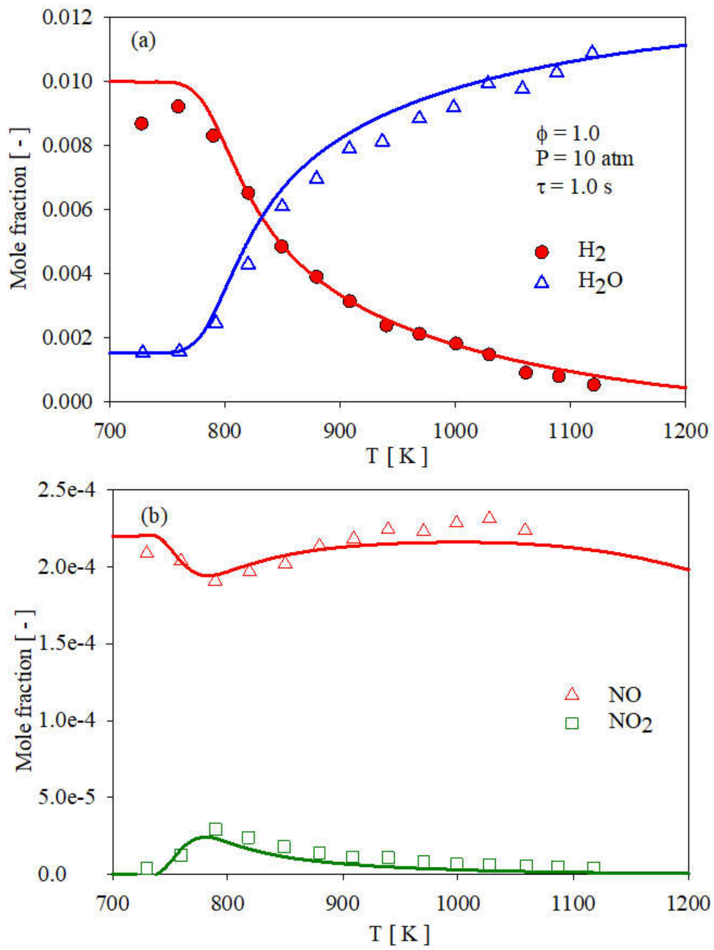

Figure S30: Speciation in during $H_2/O_2/N_2/NO$ oxidation in jet stirred reactor at $\phi = 1.0$, 10 atm and $\tau = 1.0$ s. Symbols: experiments from [20], Lines: this work

5. Burner stabilized flames

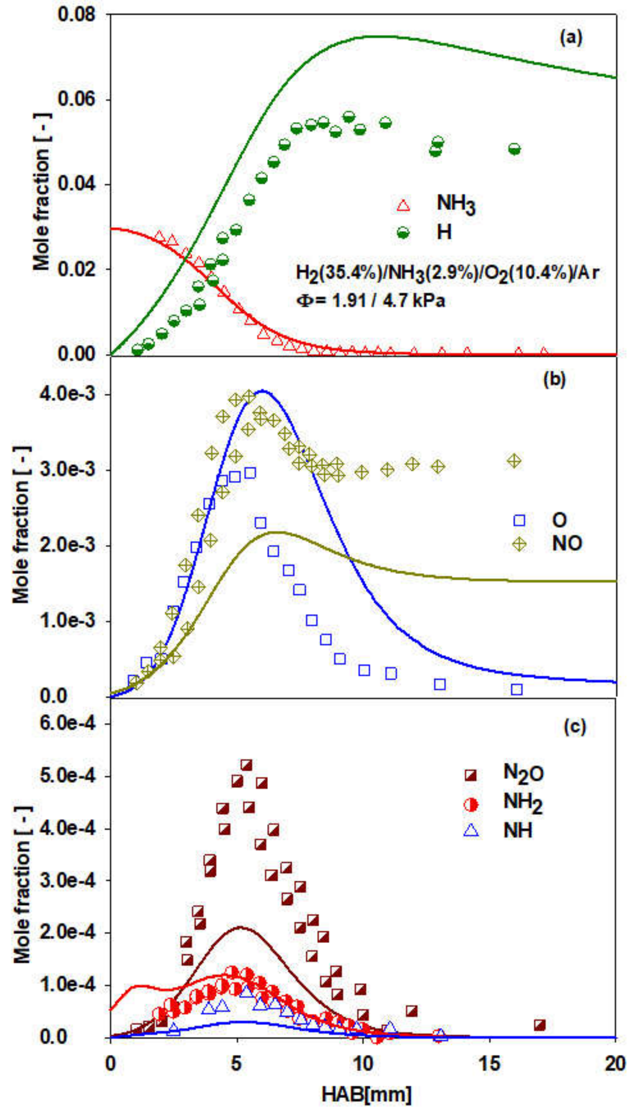

Figure S31: Speciation in $H_2/NH_3/O_2/Ar$ in burner stabilized premixed flames at $\phi = 1.91$, 4.7 kPa. Symbols: experiments from [21], Lines: this work.

References

[1] C. Lhuillier, P. Brequigny, N. Lamoureux, F. Contino, C. Mounaïm-Rousselle, Experimental investigation on laminar burning velocities of ammonia/hydrogen/air mixtures at elevated temperatures, Fuel. 263 (2020). doi:10.1016/j.fuel.2019.116653.

[2] K.P. Shrestha, L. Seidel, T. Zeuch, F. Mauss, Detailed Kinetic Mechanism for the Oxidation of Ammonia Including the Formation and Reduction of Nitrogen Oxides, Energy & Fuels. 32 (2018) 10202−10217. doi:10.1021/acs.energyfuels.8b01056.

[3] X. Han, Z. Wang, M. Costa, Z. Sun, Y. He, K. Cen, Experimental and kinetic modeling study of laminar burning velocities of NH3/air, NH3/H2/air, NH3/CO/air and NH3/CH4/air premixed flames, Combust. Flame. 206 (2019) 214–226. doi:10.1016/j.combustflame.2019.05.003.

[4] A. Hayakawa, T. Goto, R. Mimoto, Y. Arakawa, T. Kudo, H. Kobayashi, Laminar burning velocity and Markstein length of ammonia/air premixed flames at various pressures, Fuel. 159 (2015) 98–106. doi:10.1016/j.fuel.2015.06.070.

[5] P. Kumar, T.R. Meyer, Experimental and modeling study of chemical-kinetics mechanisms for H 2-NH3-air mixtures in laminar premixed jet flames, Fuel. 108 (2013) 166–176. doi:10.1016/j.fuel.2012.06.103.

[6] A. Ichikawa, A. Hayakawa, Y. Kitagawa, K.D. Kunkuma Amila Somarathne, T. Kudo, H. Kobayashi, Laminar burning velocity and Markstein length of ammonia/hydrogen/air premixed flames at elevated pressures, Int. J. Hydrogen Energy. 40 (2015) 9570–9578. doi:10.1016/j.ijhydene.2015.04.024.

[7] T. Jabbour, D.F. Clodic, Burning velocity and refrigerant flammability classification, ASHRAE Trans. 110 (2004) 522–533.

[8] K. Takizawa, A. Takahashi, K. Tokuhashi, S. Kondo, A. Sekiya, Burning velocity measurements of nitrogen-containing compounds, J. Hazard. Mater. 155 (2008) 144–152. doi:10.1016/j.jhazmat.2007.11.089.

[9] U.J. Pfahl, M.C. Ross, J.E. Shepherd, K.O. Pasamehmetoglu, C. Unal, Flammability limits, ignition energy, and flame speeds in H2-CH4-NH3- N2O-O2-N2 mixtures, Combust. Flame. 123 (2000) 140–158. doi:10.1016/S0010-2180(00)00152-8.

[10] V.F. Zakaznov, L.A. Kursheva, Z.I. Fedina, Determination of normal flame velocity and critical diameter of flame extinction in ammonia-air mixture, Combust. Explos. Shock Waves. 14 (1978) 710–713. doi:10.1007/BF00786097.

[11] Y. Li, M. Bi, B. Li, W. Gao, Explosion behaviors of ammonia–air mixtures, Combust. Sci. Technol. 190 (2018) 1804–1816. doi:10.1080/00102202.2018.1473859.

[12] P.D. Ronney, Effect of Chemistry and Transport Properties on Near-Limit Flames at Microgravity, Combust. Sci. Technol. 59 (1988) 123–141. doi:10.1080/00102208808947092.

[13] B. Mei, X. Zhang, S. Ma, M. Cui, H. Guo, Z. Cao, Y. Li, Experimental and kinetic modeling investigation on the laminar flame propagation of ammonia under oxygen

enrichment and elevated pressure conditions, Combust. Flame. 210 (2019) 236–246. doi:10.1016/j.combustflame.2019.08.033.

[14] P. Glarborg, J.A. Miller, B. Ruscic, S.J. Klippenstein, Modeling nitrogen chemistry in combustion, Prog. Energy Combust. Sci. 67 (2018) 31–68. doi:10.1016/j.pecs.2018.01.002.

[15] J. Otomo, M. Koshi, T. Mitsumori, H. Iwasaki, K. Yamada, Chemical kinetic modeling of ammonia oxidation with improved reaction mechanism for ammonia/air and ammonia/hydrogen/air combustion, Int. J. Hydrogen Energy. 43 (2018) 3004–3014. doi:10.1016/j.ijhydene.2017.12.066.

[16] A. Stagni, C. Cavallotti, S. Arunthanayothin, Y. Song, O. Herbinet, F. Battin-Leclerc, T. Faravelli, An experimental, theoretical and kinetic-modeling study of the gas-phase oxidation of ammonia, React. Chem. Eng. 5 (2020) 696–711. doi:10.1039/c9re00429g.

[17] B. Shu, S.K. Vallabhuni, X. He, G. Issayev, K. Moshammer, A. Farooq, R.X. Fernandes, A shock tube and modeling study on the autoignition properties of ammonia at intermediate temperatures, Proc. Combust. Inst. 37 (2019) 205–211. doi:10.1016/j.proci.2018.07.074.

[18] O. Mathieu, E.L. Petersen, Experimental and modeling study on the high-temperature oxidation of Ammonia and related NOx chemistry, Combust. Flame. 162 (2015) 554–570. doi:10.1016/j.combustflame.2014.08.022.

[19] X. He, B. Shu, D. Nascimento, K. Moshammer, M. Costa, R.X. Fernandes, Auto-ignition kinetics of ammonia and ammonia/hydrogen mixtures at intermediate temperatures and high pressures, Combust. Flame. 206 (2019) 189–200. doi:10.1016/j.combustflame.2019.04.050.

[20] G. Dayma, P. Dagaut, Effects of air contamination on the combustion of hydrogen-effect of NO and NO2 addition on hydrogen ignition and oxidation kinetics, Combust. Sci. Technol. 178 (2006) 1999–2024. doi:10.1080/00102200600793171.

[21] J. Vandooren, Comparison of the Experimental Structure of an Ammonia Seeded Rich Hydrogen Oxygen Argon Flame With the Calculated Ones Along Several Reaction-Mechanisms, Combust. Sci. Technol. 84 (1992) 335–344. doi:10.1080/00102209208951861.